

2026

Development of ion-loaded polyethylene glycol-based biomaterials for the controlled mineral occlusion and antibacterial sealing in dentinal tubules

Tai-Wei Feng

Ming-Fa Hsieh

Shiuh-Tzung Liu

Chun-Pin Lin

Follow this and additional works at: <https://jds.ads.org.tw/journal>

Recommended Citation

Feng, Tai-Wei; Hsieh, Ming-Fa; Liu, Shiuh-Tzung; and Lin, Chun-Pin (2026) "Development of ion-loaded polyethylene glycol-based biomaterials for the controlled mineral occlusion and antibacterial sealing in dentinal tubules," *Journal of Dental Sciences*: Vol. 21: Iss. 2, Article 39.

Available at: <https://jds.ads.org.tw/journal/vol21/iss2/39>

This Original Article is brought to you for free and open access by Journal of Dental Sciences. It has been accepted for inclusion in Journal of Dental Sciences by an authorized editor of Journal of Dental Sciences. For more information, please contact cpchiang@ntu.edu.tw.



Available online at <https://jds.ads.org.tw/journal/>

Digital Commons

journal homepage: <https://jds.ads.org.tw/journal/>



Original Article

Development of ion-loaded polyethylene glycol-based biomaterials for the controlled mineral occlusion and antibacterial sealing in dentinal tubules

Tai-Wei Feng ^a, Ming-Fa Hsieh ^b, Shih-Tzung Liu ^c,
Chun-Pin Lin ^{d,e,f*}

^a Graduate Institute of Oral Biology, School of Dentistry, National Taiwan University, Taipei, Taiwan

^b Department of Biomedical Engineering, Chung Yuan Christian University, Taoyuan, Taiwan

^c Department of Chemistry, National Taiwan University, Taipei, Taiwan

^d Graduate Institute of Clinical Dentistry, School of Dentistry, National Taiwan University, Taipei, Taiwan

^e Department of Dentistry, National Taiwan University Hospital, College of Medicine, National Taiwan University, Taipei, Taiwan

^f School of Dentistry, College of Dental Medicine, Kaohsiung Medical University, Kaohsiung, Taiwan

Received 14 November 2025

Available online 1 April 2026

KEYWORDS

Dentin sensitivity;
Biom mineralization;
Polyethylene glycols;
Nanomaterials;
Antimicrobial activity

Abstract *Background/purpose:* Dentinal tubule exposure leads to dentin hypersensitivity and pulp bacterial invasion. This study aimed to evaluate polyethylene glycol (PEG) derivatives, varying in different molecular weights (MWs) and functional groups, to achieve deep dentinal tubule occlusion and concurrent antimicrobial activity under the neutral, non-destructive conditions.

Materials and methods: PEG derivatives were synthesized, ion-loaded, and characterized. *In vitro* ion permeation and precipitation actions were assessed across various pH levels by human dentin slices and turbidity assays. The sealing depth and crystal phase of the precipitates were analyzed using scanning electron microscopy (SEM) and X-ray diffraction (XRD), respectively. Furthermore, the materials' biocompatibility, biom mineralization potential, and antibacterial activity were evaluated.

Results: Low MW PEG exhibited ideal nanoscopic size and charge neutrality. Both MW and functional group modifications affected ion permeation and controlled crystallization. Among the materials, PEG₂₀₀ group achieved the superior dentinal tubule sealing depth. However, both

* Corresponding author. Department of Dentistry, National Taiwan University Hospital, No. 1, Changde St., Zhongzheng Dist., Taipei 10048, Taiwan.

E-mail address: chunpinlin@gmail.com (C.-P. Lin).

<https://doi.org/10.1016/j.jds.2025.11.016>

1991-7902/© 2026 Association for Dental Sciences of the Republic of China. Publishing services by Digital Commons. This is an open access article under the CC BY-NC-ND license (<http://creativecommons.org/licenses/by-nc-nd/4.0/>).

the caprolactone (CL) and acrylic acid (AAC) terminal modifications significantly compromised the sealing depth. For biocompatibility, PEG and PEG-CL demonstrated excellent cytocompatibility, whereas the introduction of AAC resulted in cytotoxicity. Regarding antimicrobial performance, Low MW PEG and AAC group showed broad-spectrum antimicrobial efficacy. **Conclusion:** PEG derivatives with low MW are the most promising candidates, demonstrating excellent biocompatibility and deep dentinal tubule sealing via strontium phosphate-related crystallization under the neutral conditions. While functional groups like AAC offer superior crystal control and antibacterial properties, the associated reduced penetration depth and cytotoxicity necessitate further optimization for clinical application.

© 2026 Association for Dental Sciences of the Republic of China. Publishing services by Digital Commons. This is an open access article under the CC BY-NC-ND license (<http://creativecommons.org/licenses/by-nc-nd/4.0/>).

Introduction

Dentinal tubule exposure is a key factor resulting in dentin hypersensitivity¹ and bacterial invasion of the pulp, which often leads to pulpitis and endodontic failure.² Therefore, effective and lasting strategies for dentinal tubule occlusion are necessary.

Despite our previous study demonstrated that bioactive formulations, like DP-Bioglass³ and Ca@mesoporous silica,⁴ successfully promote intratubular mineralization. These systems shared the same clinical limitations with commercial products: The requirement of acidic environment or prolonged reaction time.⁵

Consequently, we proposed to utilize polyethylene glycol (PEG) and its derivatives as a novel strategy for intradentinal ion delivery and biomineralization in this study. PEG-based biomaterials are considered ideal carriers due to their multiple advantages: Their surface brush-like structure effectively shields ionic charges,⁶ ensuring the rapid and deep delivery of substances into the dentinal tubules. Second, their osmotic effect could prevent premature material aggregation⁷ and serve as a template for guided crystallization.⁸ Furthermore, PEG has been demonstrated to possess antimicrobial properties.⁹ The use of lipophilic end-groups, such as caprolactone (CL), can enhance PEG's stability in aqueous environments,¹⁰ while acrylic acid (AAC) is commonly employed in dental curing systems.¹¹

This study evaluated PEG derivatives with varying molecular weights and functional groups, encapsulating alkaline earth metal ions, and also investigated the mechanism. Our goal was to achieve controlled ion delivery into the deeper dentinal tubules under the neutral, non-destructive conditions for tooth structure, resulting in deep precipitation and occlusion while simultaneously exerting antimicrobial capability.

Materials and methods

Synthesis and characterization of PEG and its derivatives

We synthesized a series of different PEG derivatives, varying the molecular weight (MW) from 200 to 5000 Da. All reagents

used in this study were purchased from Sigma (Sigma–Aldrich, St. Louis, MO, USA). PEG-CL was synthesized by grafting ϵ -caprolactone onto the PEG via ring opening polymerization, following the method by Hossein et al.¹² The reaction was conducted at 130 °C, catalyzed by stannous octoate. The resultant product was purified in chloroform, precipitation with cold diethyl ether. Subsequently, the PEG-CL-AAC product was prepared following Zhang et al.:¹³ PEG-CL was dissolved in chloroform and reacted with triethylamine and acryloyl chloride. The final product was obtained after dialysis and freeze-drying. The structure of the products was confirmed using Fourier transform infrared spectroscopy (FTIR) (JASCO Corporation, Tokyo, Japan) and proton nuclear magnetic resonance (¹H NMR) (Bruker Corporation, Billerica, MA, USA) spectroscopy. For ion loading, the PEG and its derivations were dissolved at 5 wt% in 50 mM calcium chloride or strontium chloride solutions. The solutions' pH was adjusted to 3, 7, and 9. The particle size and surface potential were measured using Zetasizer Ultra (Malvern Panalytical, Malvern, Worcestershire, UK).

Dentin specimen preparation and ion permeation

Healthy adults' third molars extracted for clinical reasons were collected (IRB: 202104099RIND, National Taiwan University Hospital). Samples with caries, cracks, restorations, or prior endodontic treatment were excluded. Occlusal enamel was removed using a low-speed diamond saw (ISOMET, Buehler, Lake Bluff, IL, USA), and 500 μ m dentin discs were sectioned from the cervical area. To remove the smear layer and organic components, discs were treated with 5 % sodium hypochlorite for 60 s and then etched with phosphoric acid gel (Kerr Corporation, Brea, CA, USA) for 30 s, followed by rinsing and air-drying. To ensure a consistent contact area, each dentin disc was bonded to a 4 mm diameter custom plastic cylinder using flowable light-cured resin (Tokuyama Dental Corporation, Tokyo, Japan). Additional resin was applied along the margins. The specimen was mounted on Millicell® inserts (Merck KGaA, Darmstadt, Germany).

A 200 μ L of test solution was added to the donor chamber, and 1 mL of deionized water to the receiver. Samples from the receiver chamber were collected at defined time points, with the withdrawn volume immediately replaced by a same

volume of fresh deionized water. Ion concentrations were quantified using commercial colorimetric detection kits (Biovision Inc., Milpitas, CA, USA).

Precipitation behavior

The precipitation behavior under varying pH conditions was semi-quantitatively by turbidity assay. 50 μ L of the test solution was dispensed into a 96-well plate, and 50 μ L of pH-adjusted phosphate-buffered saline was added. The resulting mixtures were incubated at 37 $^{\circ}$ C. Changes in

absorbance at 595 nm were recorded to continuously monitor the precipitation kinetics.

Dentinal tubule sealing assessment and crystal phase analysis

The test materials were applied to the upper surface of the dentin slices and allowed to react for 24 h at 37 $^{\circ}$ C. Following the reaction, the specimens were washed with deionized water to remove the residual materials. After freeze drying, the specimens were sectioned and examined

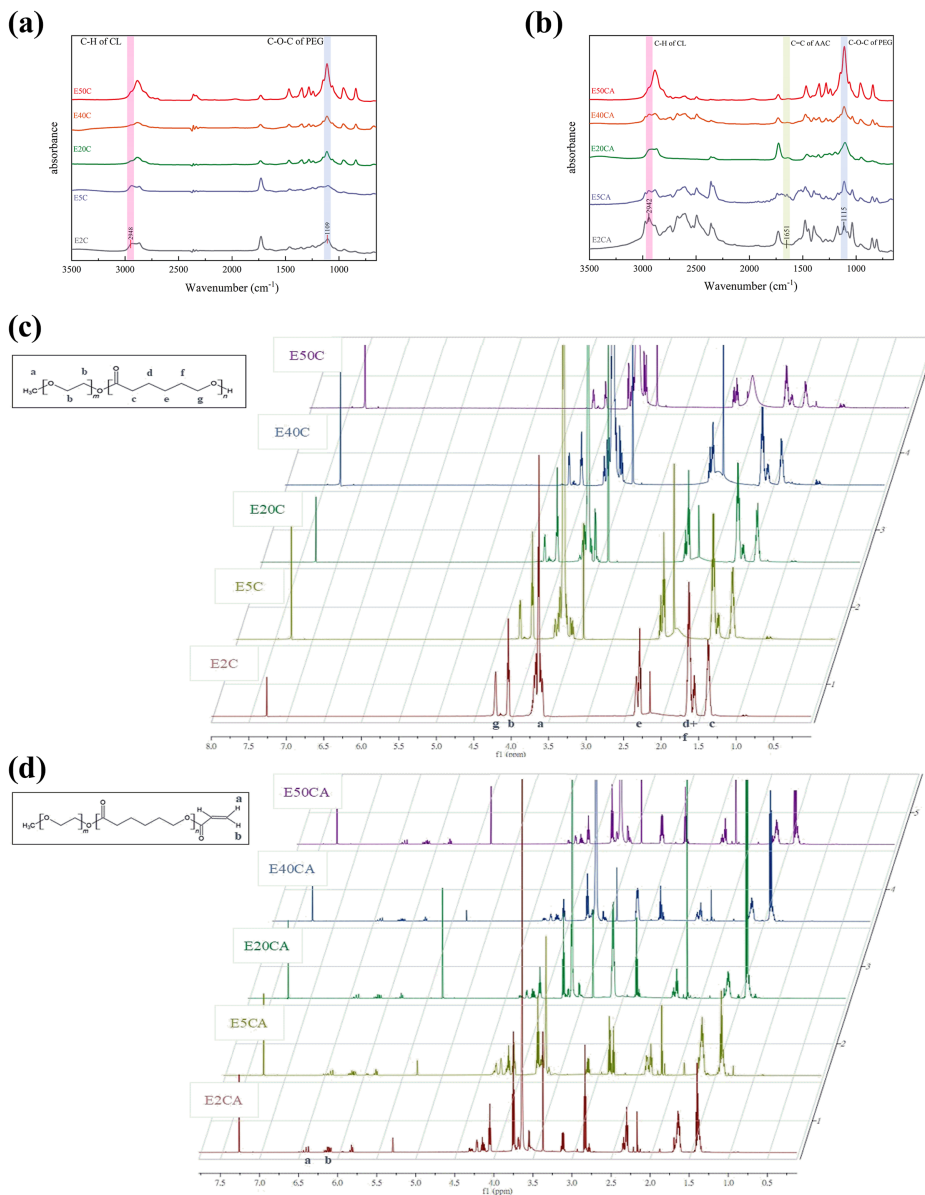


Figure 1 Structural characterization of polyethylene glycol (PEG) derivatives. The structural properties of the synthesized PEG-caprolactone (PEG-CL) and PEG-CL-acrylic acid (PEG-CL-AAC) derivatives were confirmed using spectroscopy. Fourier-transform infrared spectroscopy (FTIR) spectra for PEG-CL and PEG-CL-AAC are shown in (a) and (b), respectively. The corresponding ¹H nuclear magnetic resonance (¹H NMR) spectra are presented in (c) for PEG-CL and (d) for PEG-CL-AAC. The samples are designated based on the molecular weight of the modifying PEG: E2C, E5C, E20C, E40C, and E50C represent CL modified with 200, 550, 2000, 4000, and 5000 Da PEG (PEG-CL), respectively. The samples E2CA, E5CA, E20CA, E40CA, and E50CA represent the corresponding CL-AAC derivatives obtained from PEG-modified CL with 200, 550, 2000, 4000, and 5000 Da PEG, respectively.

using scanning electron microscopy (SEM) (Hitachi High-Tech Corporation, Tokyo, Japan) to observe the sealing depth within the dentinal tubules.

X-ray diffraction (XRD) (Bruker AXS, Madison, WI, USA) was employed to identify the crystal phase of the precipitates. The analysis was conducted under the same experimental conditions as the predetermined ion species and environmental pH values. The XRD scanning range was set from 5° to 50° at a rate of 10°/minutes. Phase identification was performed using Highscore V3.0e (Malvern Analytical, Almelo, The Netherlands).

Biocompatibility, biomineralization induction and antibacterial assays

NIH/3T3 mouse embryonic fibroblasts (BCRC, Hsinchu, Taiwan) were cultured in DMEM-HG supplemented with 4 mM L-glutamine, 1 % non-essential amino acids, 1 % antibiotics, and 10 % fetal bovine serum (Corning Incorporated, Kennebunk, ME, USA). Cells were seeded in 96-well plates at a density of 1.0×10^4 cells/well and subsequently exposed to culture media containing 10 wt% of the test sample for 1 day. Cell viability and cytotoxicity were assessed by CCK-8 assay and LDH assay kit (Dojindo Laboratories, Kumamoto, Japan).

Human dental pulp stem cells, sourced from National Taiwan University Hospital, were seeded in 48-well plates at 1.0×10^5 cells/well and treated for 21 days. Cell proliferation was measured by CCK-8 assay. Alkaline

phosphatase (ALP) activity was determined using the ALP substrate (Sigma–Aldrich). Matrix mineralization was evaluated by using Alizarin red S (ARS) staining and cetylpyridinium chloride (Sigma–Aldrich).

Antibacterial activity was assessed against *Escherichia coli* and *Staphylococcus aureus* (BCRC, Hsinchu, Taiwan), cultured in tryptic soy broth (Himedia Laboratories Pvt. Ltd., Mumbai, Maharashtra, India). After adding 10 % of the sample to the medium and incubating for one day, total bacterial amount was measured by optical density and viability by CCK-8 assay.

Statistical analysis

All results are expressed as mean \pm standard deviation. The ANOVA followed by Tukey's post hoc test was performed by SPSS v20.0 (IBM Corporation, Armonk, NY, USA), with significance set at $P < 0.05$. Thresholds were denoted as * $P < 0.05$, ** $P < 0.01$, and *** $P < 0.001$.

Results

Characterization of PEG and its derivatives

The synthesis of the PEG derivatives was verified through spectroscopic analysis. The FTIR spectrum (Fig. 1a) confirmed the successful grafting of CL via characteristic absorption peaks at 1730 cm^{-1} and 2950 cm^{-1} , corresponding to the C=O double bond and C–H stretching. In

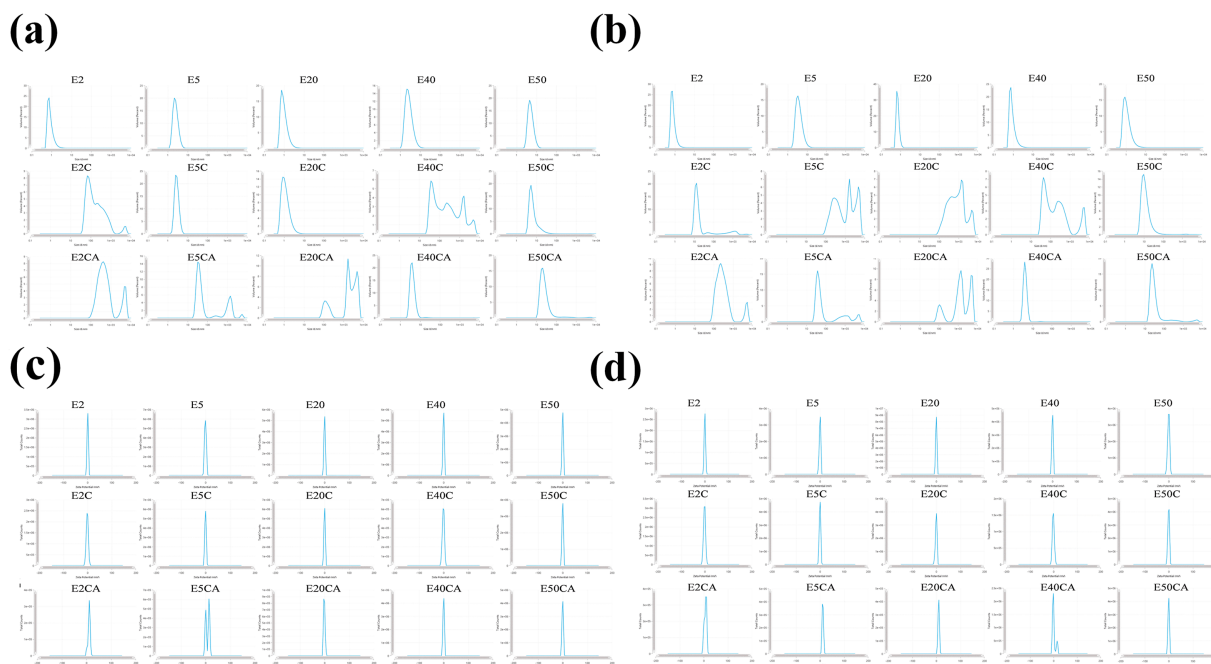


Figure 2 The physicochemical properties of the synthesized polyethylene glycol (PEG) derivatives as determined by dynamic light scattering analysis. Panels (a) (Calcium group) and (b) (Strontium group) show the particle size distributions of the sample series, while Panels (c) (Calcium group) and (d) (Strontium group) display the corresponding Zeta potentials, respectively. The sample designations are based on the molecular weight of the modifying PEG: E2, E5, E20, E40, and E50 represent PEG molecular weights of 200, 550, 2000, 4000, and 5000 Da, respectively. Specifically, the EC series (e.g., E2C, E5C, E20C ...) represents the CL derivatives modified with PEG (PEG-CL), and the ECA series (e.g., E2CA, E5CA, E20CA ...) represents the corresponding CL-AAC derivatives obtained from the PEG-modified CL precursors.

the PEG-CL-AAC spectrum (Fig. 1b), the new vibrational absorption at 1650 cm^{-1} confirmed the presence of the C=C double bond from the acrylic acid structure. $^1\text{H NMR}$ analysis further validated the chemical structures: the 1.37–4.03 ppm signals in PEG-CL (Fig. 1c) confirmed CL integration, while the multiplet signals at 6.1 and 6.4 ppm corresponding to the vinylic protons in PEG-CL-AAC (Fig. 1d) confirmed the successful acrylation.

The ion-loaded materials underwent particle characterization (Fig. 2). The surface potential of all PEG and its derivative materials remained charge-neutral. The non-modified PEG group exhibited ideal nanoscopic properties, showing a stable, monodisperse size distribution with particle sizes below 10 nm. The PEG-CL group, as micelle-like structure, the particle size increased but still remained within the nanometer scale. Conversely, the PEG-CL-AAC group, the double bond stereo-structure led to an unstable, polydisperse size distribution, causing the particle size to increase to the near-micrometer scale.

Effects of PEG derivatives on *in vitro* dentin permeation and precipitation behavior

In general, PEG and their derivatives exhibited similar trends in the dentin permeation profile (Fig. 3). The acidic conditions consistently demonstrated significantly superior permeation capacity. Regarding MW, materials with a lower MW exhibited relatively favorable penetrability. Furthermore, those with functional group modifications were found to markedly enhance the ion permeation.

The turbidity analysis in Fig. 4 presented a generally inverse relationship to the permeation profile. The mode of precipitation was highly dependent on pH, with alkaline conditions being relatively conducive to crystal formation. The higher MW groups exhibited a greater total change in turbidity, suggesting superior overall precipitation quantity or enhanced control over crystallization. Furthermore, consistent with the permeation results, terminal functional

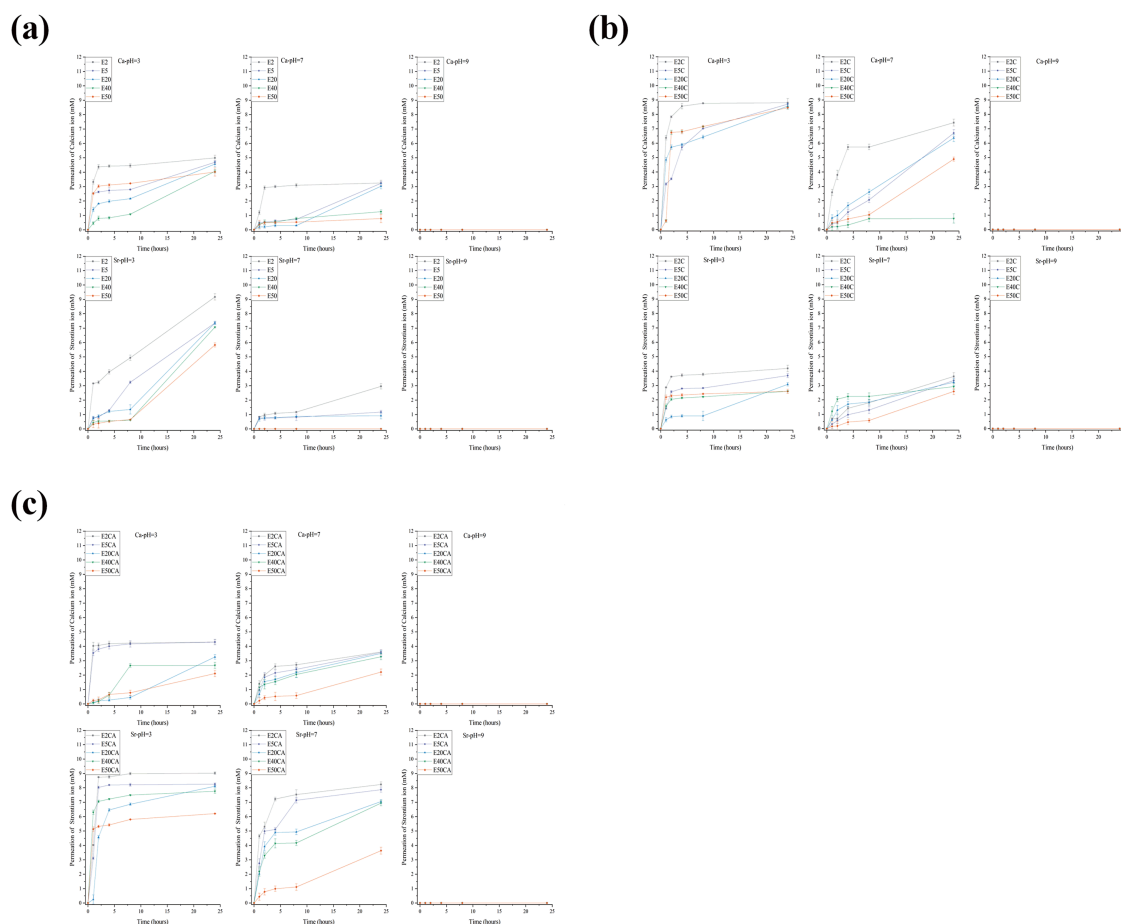


Figure 3 The permeation profile of different polyethylene glycol (PEG)-based biomaterials carrying either calcium or strontium ions into human dentin disc model. The panels compare the results for three material types based on their chemical structure: (a) Unmodified PEG, (b) PEG-caprolactone (PEG-CL) derivatives (EC series), and (c) PEG-CL-acrylic acid (PEG-CL-AAC) derivatives (ECA series). The sample nomenclature reflects the molecular weight of the modifying PEG: E2, E5, E20, E40, and E50 correspond to PEG molecular weights of 200, 550, 2000, 4000, and 5000 Da, respectively. The EC series represents the CL derivatives modified with PEG (PEG-CL), while the ECA series represents the corresponding CL-AAC derivatives synthesized from the PEG-modified CL precursors.

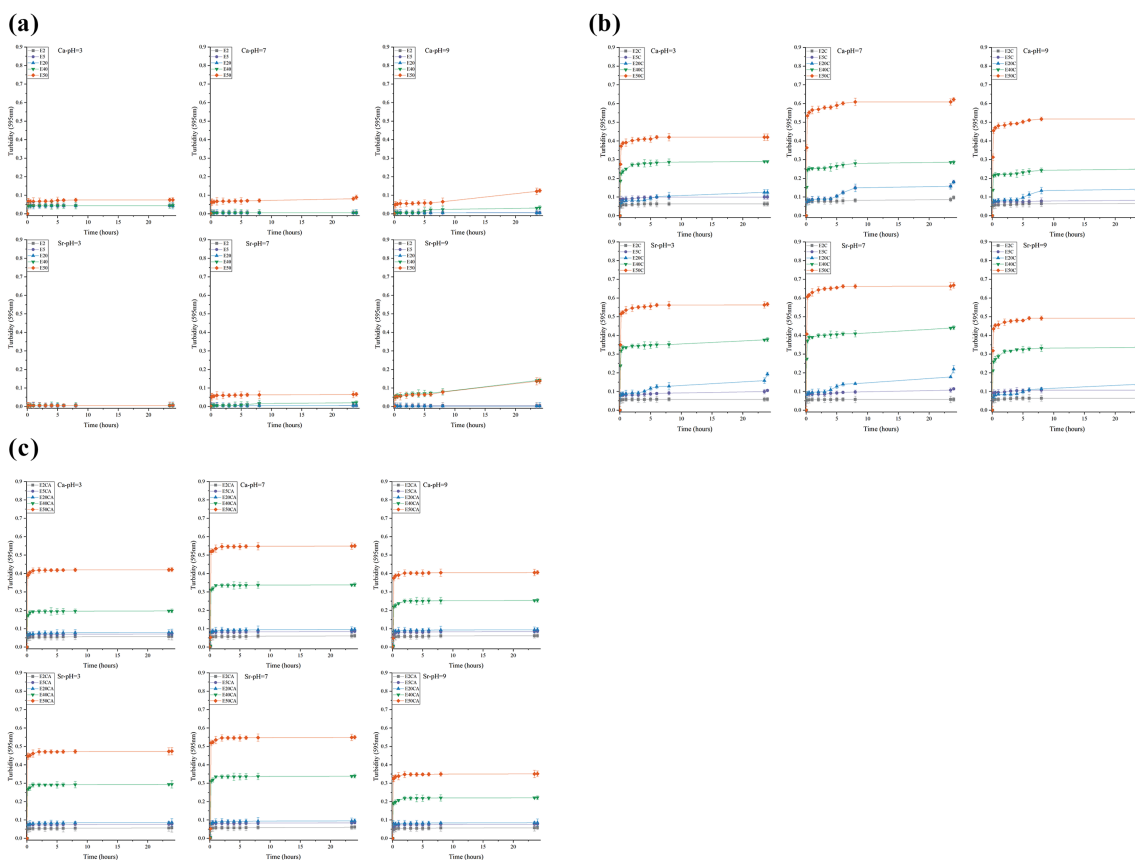


Figure 4 The turbidity changes of different polyethylene glycol (PEG)-based biomaterials carrying either calcium or strontium ions. The panels compare the results for three material types based on their chemical structure: (a) Unmodified PEG, (b) PEG-caprolactone (PEG-CL) derivatives (EC series), and (c) PEG-CL-acrylic acid (PEG-CL-AAC) derivatives (ECA series). The sample nomenclature reflects the molecular weight of the modifying PEG: E2, E5, E20, E40, and E50 correspond to PEG molecular weights of 200, 550, 2000, 4000, and 5000 Da, respectively. The EC series represents the CL derivatives modified with PEG (PEG-CL), while the ECA series represents the corresponding CL-AAC derivatives synthesized from the PEG-modified CL precursors.

group modifications also significantly increased the total turbidity change, indicating that these modifications not only influence permeation but also optimize the material's capacity for crystal generation.

Sealing ability of PEG derivatives in dentinal tubules and its crystal phase

The sealing ability of PEG₂₀₀ and its derivative materials that simultaneously induced Sr²⁺ penetration and crystal precipitation was investigated in this study. Fig. 5 demonstrated that the PEG without modification exhibited the most superior sealing depth: approximately 140 μm under pH = 3 and 90 μm under pH = 7. However, in the group with CL, the sealing depth began to gradually diminish. The depth decreased from approximately 80 μm–50 μm. Moreover, the sealing capability of PEG-CL-AAC group was substantially restricted. In both cases, precipitation was limited to a shallow sealing layer, only within a depth range of 10 μm.

We further analyzed the crystal type of these group. Fig. 4b confirmed that these materials primarily resulted in the formation of strontium hydrogenphosphate-related crystals, specifically including strontium hydrogenphosphate¹⁴ and strontium-apatite.¹⁵

The biocompatibility analysis

The biocompatibility analysis (Fig. 6a–b) demonstrated that both the PEG and PEG-CL groups exhibited excellent cytocompatibility, effectively classifying them as non-toxic materials. However, the results simultaneously indicated that the introduction of acrylic acid as a modifier imparted a degree of cytotoxicity. This reduction was particularly pronounced in formulations utilizing a high MW group, leading to significant cell death.

Considering PEG₂₀₀ and its derivative materials as the primary focus of this study, their effects on stem cells were further investigated (Fig. 6c–e). Our findings revealed that all groups possessed the ability to induce cell proliferation, and to promote early-stage mineralization and late-stage calcification. Among these materials, the PEG group exhibited the most favorable overall performance.

Fig. 7 illustrates the antibacterial efficacy of these materials. Low MW groups effectively inhibited the growth of both bacterial strains, whereas higher MW groups exhibited only negligible inhibitory effects. Furthermore, the CL modification showed no enhancement of the antibacterial effect. In contrast, the incorporation of AAC demonstrated a potent bactericidal ability specifically against *S. aureus*.

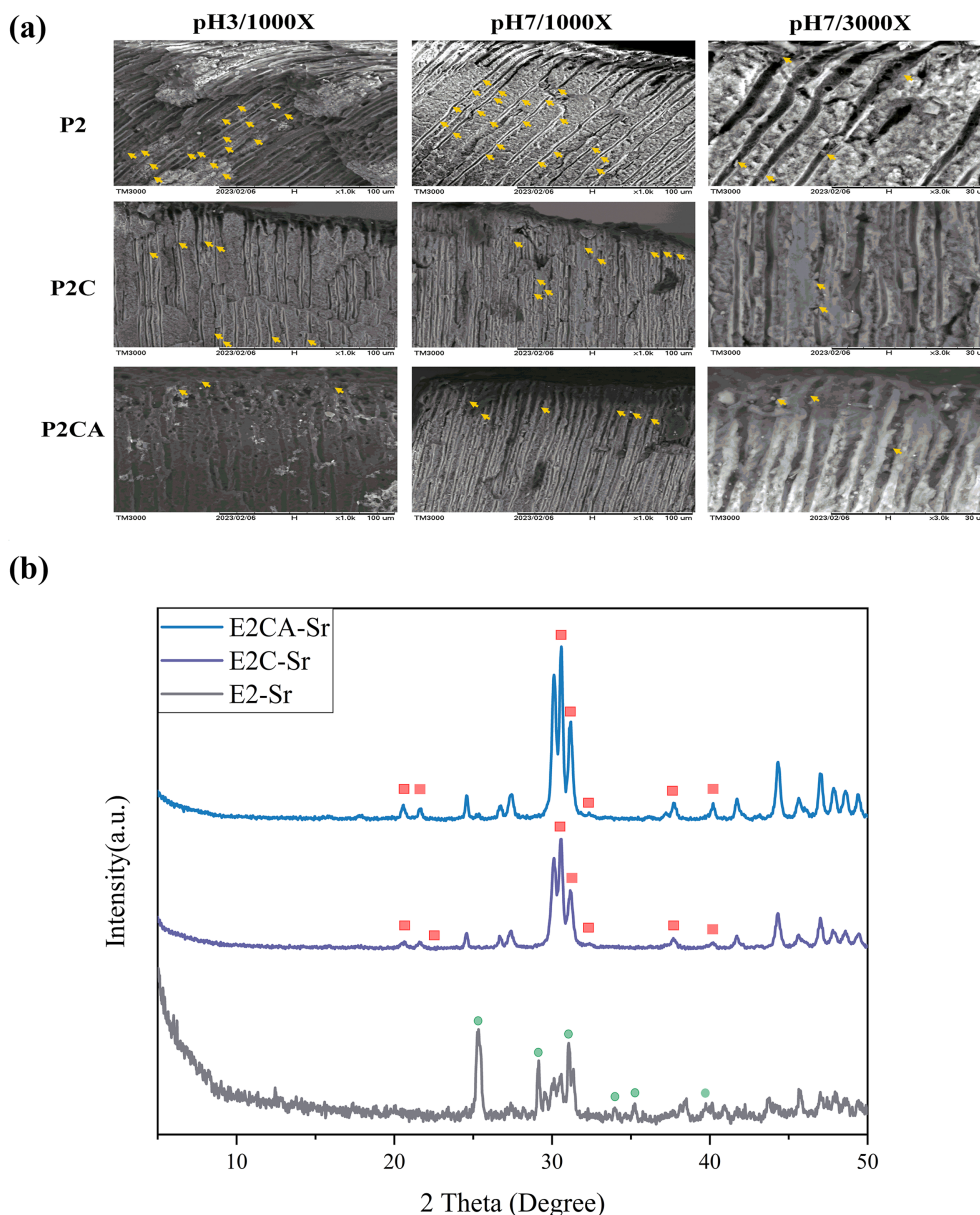


Figure 5 The sealing ability of the polyethylene glycol (PEG) derivatives within dentinal tubules and the crystal phases formed after treatment. Panel (a) shows the scanning electron microscopy (SEM) morphology of the treated dentin surface. The yellow arrows indicate regions where crystallization has occurred. The scale bars used are 100 μm for the 1000 \times magnification image and 30 μm for the 3000 \times magnification image. Panel (b) presents the X-ray diffraction (XRD) crystal phase analysis results. Characteristic peaks for strontium hydrogenphosphate are marked by green circles, and characteristic peaks for strontium-apatite are marked by red squares. The sample designations are based on PEG molecular weight and modification: E2 represents PEG with a molecular weight of 200 Da; E2C represents the derivative obtained by modifying caprolactone (CL) with E2; and E2CA represents the derivative obtained by further modifying E2C with acrylic acid (AAC).

Discussion

Optimized ion-carrying PEG derivatives are introduced as nanoscale biomaterials for deep dentinal tubule occlusion. By utilizing their neutral surface and potent antimicrobial activity, these derivatives facilitate deep permeation and Sr^{2+} -induced crystallization under mild conditions. This represents an effective, non-destructive, and biocompatible strategy for dentinal tubule occlusion.

Dentinal tubule permeation of biomedical agents is selectively dependent on molecular size; specifically, the diffusion coefficient decreases as molecular size increases.^{16,17} Consistent with this principle, our findings confirmed that for PEG biomaterials with similar backbone structures but varying chain lengths and functional groups, lower MW correlated with superior penetrability.

Molecular weight and functional groups are critical factors governing the rapid crystal formation mediated by

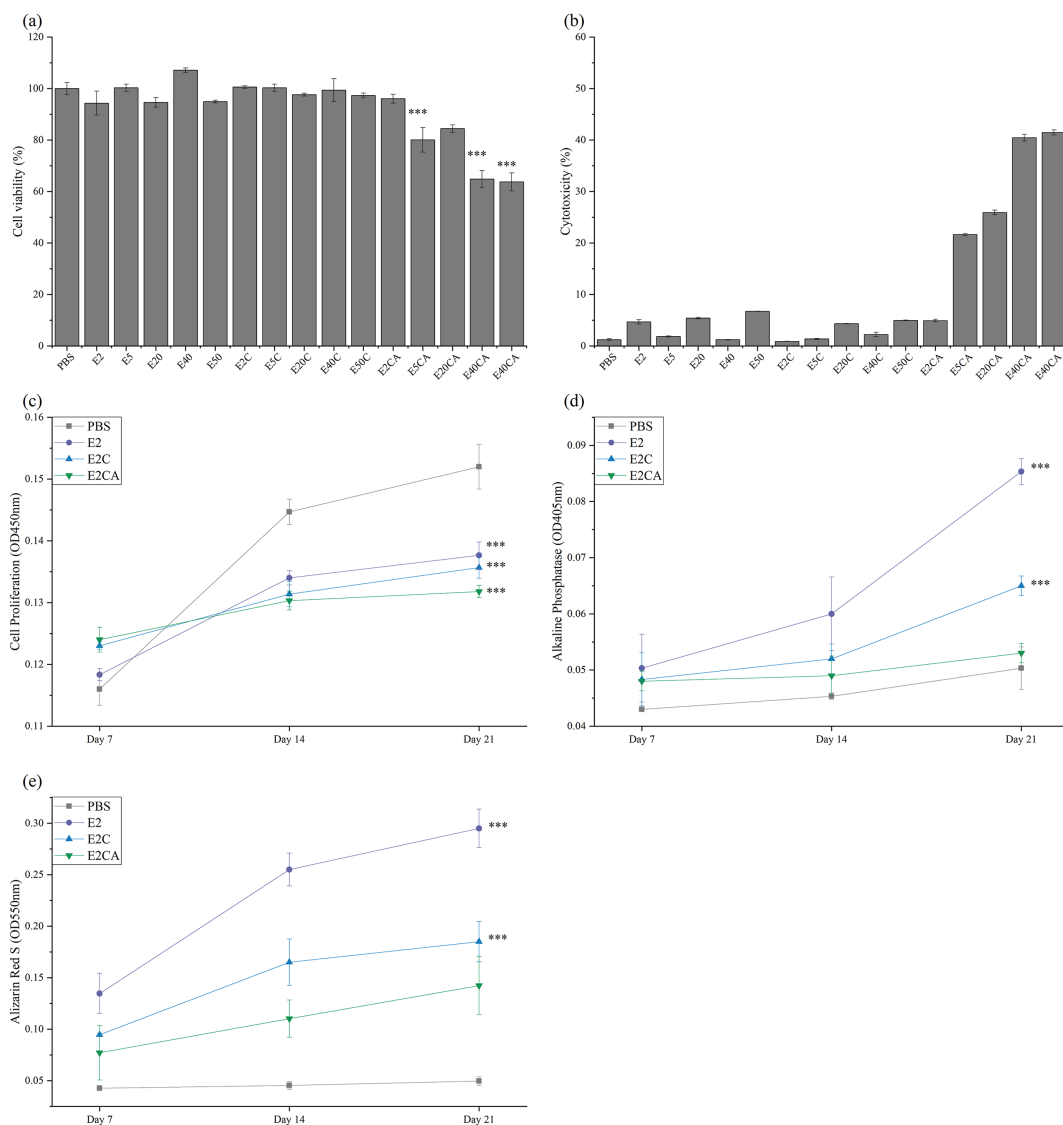


Figure 6 The cytocompatibility and mineralization capacity of polyethylene glycol (PEG) derivatives. The panels illustrate various biological outcomes: (a) Cell viability, (b) Cytotoxicity, (c) Cell proliferation, (d) Early cellular mineralization, and (e) Late cellular calcification. The sample nomenclature reflects the molecular weight of the modifying PEG: E2, E5, E20, E40, and E50 correspond to PEG molecular weights of 200, 550, 2000, 4000, and 5000 Da, respectively. The EC series represents the caprolactone (CL) derivatives modified with PEG (PEG-CL), while the ECA series represents the corresponding CL-acrylic acid (CL-AAC) derivatives synthesized from the PEG-modified CL precursors.

materials.¹⁸ Consistently, our study confirmed that the capacity to control crystal generation became more pronounced as the polymer chain length increased.¹⁹ Specifically, the long-chain group exhibited the better control, evidenced by the minimal change in solution turbidity. Besides, the superior performance of the AAC group over the CL group can be rationalized by the presence of the carboxylic acid functionality.²⁰

The SEM results revealed a critical trend: the sealing depth achieved by the crystalline precipitates significantly decreased, from an optimum of approximately 140 μm to merely 10 μm , following the terminal modification. This finding strongly suggests that the structural modification profoundly compromises the material's longitudinal penetrability within the tubules and the subsequent crystallization efficacy.

The cytocompatibility assay confirmed the expected non-toxic performance of PEG and PEG-CL, aligning with their FDA biosafety approval.²¹ Although the incorporation of AAC introduced a measurable degree of cytotoxicity,²² the critical advantage these materials is their capacity to promote hard tissue regeneration.

Our results revealed that the antimicrobial activity of the PEG derivatives was also closely associated with both their MW and terminal functionalization. Low MW PEG significantly reduced bacterial viability by employing a lytic action driven by low viscosity and high osmotic pressure,²³ whereas high MW PEG potentially conferred potent anti-biofilm activity through enhanced steric stability.²⁴ While CL paradoxically promoted the growth of select bacteria,²⁵ AAC generated a bactericidal effect via a membrane-compromising ion-exchange mechanism.²⁶

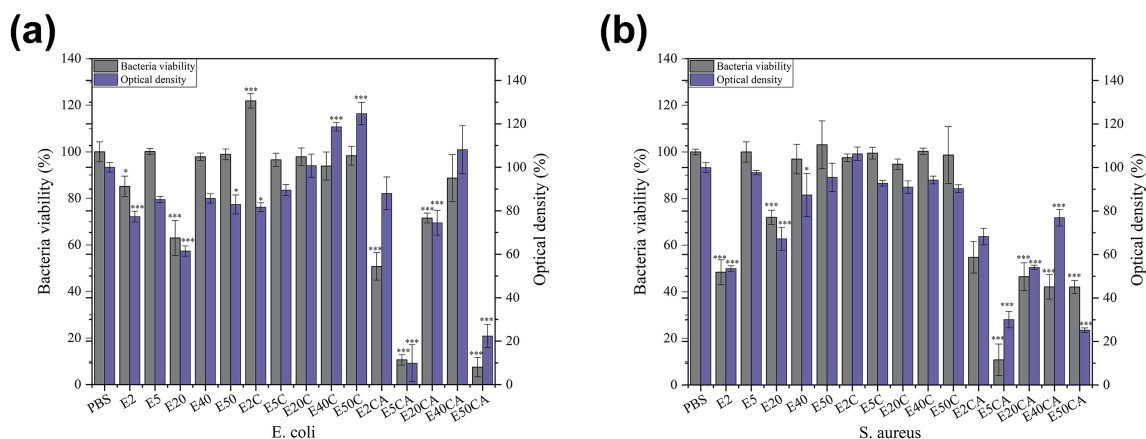


Figure 7 The antibacterial efficacy of the polyethylene glycol (PEG) derivative series against common bacterial strains. The results are presented for (a) *Escherichia coli* and (b) *Staphylococcus aureus*. The sample nomenclature utilized throughout the figure reflects the molecular weight of the modifying PEG: E2, E5, E20, E40, and E50 correspond to PEG molecular weights of 200, 550, 2000, 4000, and 5000 Da, respectively. Specifically, the EC series represents the caprolactone (CL) derivatives modified with PEG (PEG-CL), and the ECA series represents the corresponding CL-acrylic acid (CL-AAC) derivatives synthesized from the PEG-modified CL precursors.

These structure–function relationships account for the observed variations in antimicrobial capabilities among the materials.

Although the introduction of AAC demonstrated superior performance in crystal regulation and antimicrobial activity, the resulting cytotoxicity and potential inhibitory effects on intracanal crystallization presented considerable room for development. Therefore, the focus should be on developing or screening strategies that retain the functional advantages of AAC without compromising cytocompatibility. Besides, terminal modification severely compromises the material’s longitudinal penetration depth, which is a critical bottleneck for achieving deep tubule sealing. Designing functionalization strategies that do not sacrifice penetrability, such as side-chain functionalization, may offer a viable solution to this issue.

In conclusion, based on a comprehensive analysis of all aforementioned experimental factors, we ultimately screened PEG derivatives as the most promising candidates for clinical application. These materials demonstrated their suitability for the crystalline occlusion of dentinal tubules under neutral conditions. This groundbreaking work lays the essential foundation for future translational research, paving the way for integrating PEG-based systems into minimally invasive treatments for dentin hypersensitivity, bacterial ingress, and even regenerative endodontics.

Declaration of competing interest

The authors have no conflicts of interest relevant to this article.

Acknowledgments

This research was funded by research grants from National Taiwan University Hospital (111-UN0022).

References

- West NX, Lussi A, Seong J, Hellwig E. Dentin hypersensitivity: pain mechanisms and aetiology of exposed cervical dentin. *Clin Oral Invest* 2013;17(Suppl 1):S9–19.
- Stauffacher S, Lussi A, Nietzsche S, Neuhaus KW, Eick S. Bacterial invasion into radicular dentine-an in vitro study. *Clin Oral Invest* 2017;21:1743–52.
- Lee BS, Kang SH, Wang YL, Lin FH, Lin CP. In vitro study of dentinal tubule occlusion with sol-gel DP-bioglass for treatment of dentin hypersensitivity. *Dent Mater J* 2007;26: 52–61.
- Chiang YC, Lin HP, Chang HH, et al. A mesoporous silica biomaterial for dental biomimetic crystallization. *ACS Nano* 2014;8:12502–13.
- Mosquim V, Santin DC, Jacomine JC, et al. Metals, fluoride and bioactive glass on dentin hypersensitivity and quality of life: a 6-month double-blind randomized clinical trial. *J Dent* 2025; 160:105931.
- Levchenko TS, Rammohan R, Lukyanov AN, Whiteman KR, Torchilin VP. Liposome clearance in mice: the effect of a separate and combined presence of surface charge and polymer coating. *Int J Pharm* 2002;240:95–102.
- Li FJ, Zhang SD, Liang JZ, Wang JZ. Effect of polyethylene glycol on the crystallization and impact properties of polylactide-based blends. *Polym Adv Technol* 2015;26:465–75.
- Dong Y, Meng F. Effect of polyethylene glycol on crystal growth and photocatalytic activity of anatase TiO₂ single crystals. *RSC Adv* 2020;10:12511–8.
- Nalawade TM, Bhat K, Sogi SH. Bactericidal activity of propylene glycol, glycerine, polyethylene glycol 400, and polyethylene glycol 1000 against selected microorganisms. *J Int Soc Prev Community Dent* 2015;5:114–9.
- Hassankhani Rad A, Asiaee F, Jafari S, Shayanfar A, Lavasanifar A, Molavi O. Poly(ethylene glycol)-poly(ϵ -caprolactone)-based micelles for solubilization and tumor-targeted delivery of silibinin. *Bioimpacts* 2020;10:87–95.
- Van Meerbeek B, Yoshihara K, Van Landuyt K, Yoshida Y, Peumans M. From Buonocore’s pioneering acid-etch technique to self-adhering restoratives. A status perspective of rapidly advancing dental adhesive technology. *J Adhesive Dent* 2020;22: 7–34.

12. Danafar H, Khurana V. Preparation and characterization of PCL-PEG-PCL polymersomes for delivery of clavulanic acid. *Cogent Med* 2016;3:1235245.
13. Zhang J, Men K, Gu Y, et al. Preparation of core cross-linked PCL-PEG-PCL micelles for doxorubicin delivery in vitro. *J Nanosci Nanotechnol* 2011;11:5054–61.
14. Boudjada A, Masse R, Guitel JC. Structure cristalline de l'orthophosphate monoacide de strontium: SrHPO₄: forme triclinique. *Acta Crystallogr B* 1978;34:2692–5.
15. Sudarsanan K, Young RA. Structure of strontium hydroxide phosphate, Sr₅(PO₄)₃OH. *Acta Crystallogr B* 1972;28:3668–70.
16. Hanks CT, Wataha JC, Parsell RR, Strawn SE, Fat JC. Permeability of biological and synthetic molecules through dentine. *J Oral Rehabil* 1994;21:475–87.
17. Calt S, Serper A, Özçelik B, Dalat MD. pH changes and calcium ion diffusion from calcium hydroxide dressing materials through root dentin. *J Endod* 1999;25:329–31.
18. Amjad Z, Zuhl R. The influence of polymer architecture on inhibition of amorphous calcium phosphate precipitation. *Phosphorus Res Bull* 2002;13:51–7.
19. Pashley DH, Livingston MJ. Effect of molecular size on permeability coefficients in human dentine. *Arch Oral Biol* 1978;23:391–5.
20. Kamitakahara M, Kawashita M, Kokubo T, Nakamura T. Effect of polyacrylic acid on the apatite formation of a bioactive ceramic in a simulated body fluid: fundamental examination of the possibility of obtaining bioactive glass-ionomer cements for orthopaedic use. *Biomaterials* 2001;22:3191–6.
21. Dethe MR, AP, Ahmed H, Agrawal M, Roy U, Alexander A. PCL-PEG copolymer based injectable thermosensitive hydrogels. *J Contr Release* 2022;343:217–36.
22. Kurata S, Morishita K, Kawase T, Umemoto K. Cytotoxic effects of acrylic acid, methacrylic acid, their corresponding saturated carboxylic acids, HEMA, and hydroquinone on fibroblasts derived from human pulp. *Dent Mater J* 2012;31: 219–25.
23. Falghoush A, Beyenal H, Besser TE, Omsland A, Call DR. Osmotic compounds enhance antibiotic efficacy against acinetobacter baumannii biofilm communities. *Appl Environ Microbiol* 2017;83:e01297-17.
24. Jayanetti M, Thambiliyagodage C, Liyanaarachchi H, Ekanayake G, Mendis A, Usgodaarachchi L. In vitro influence of PEG functionalized ZnO–CuO nanocomposites on bacterial growth. *Sci Rep* 2024;14:1293.
25. Pompa-Monroy DA, Iglesias AL, Dastager SG, et al. Comparative study of polycaprolactone electrospun fibers and casting films enriched with carbon and nitrogen sources and their potential use in water bioremediation. *Membranes* 2022;12:327.
26. Gratzl G, Walkner S, Hild S, Hassel AW, Weber H, Paulik C. Mechanistic approaches on the antibacterial activity of poly(acrylic acid) copolymers. *Colloids Surf B Biointerfaces* 2015; 126:98–105.